American Mineralogist, Volume 93, pages 1349–1355, 2008

Crystal chemical and structural characterization of fibrous tremolite from Susa Valley, Italy, with comments on potential harmful effects on human health

PAOLO BALLIRANO,[1,2,*] GIOVANNI B. ANDREOZZI,[1,3] AND GIROLAMO BELARDI[2]

[1]Dipartimento di Scienze della Terra, Sapienza Università di Roma, P.le A. Moro, 5, I-00185 Rome, Italy
[2]CNR-IGAG, Istituto di Geologia Ambientale e Geoingegneria, Sede di Roma, Via Bolognola 7, I-00138 Rome, Italy
[3]CNR-IGG, Istituto di Geoscienze e Georisorse, Sede di Roma, P.le A. Moro, 5, I-00185 Rome, Italy

ABSTRACT

This study is part of a broad research project devoted to the "amphibole fibers environmental problem" as related to the proposed excavation of the Susa Valley railway tunnel. In this locality, tunnel excavations are planned through metamorphic formations containing amphibole asbestos minerals, and this may give rise to worker health and public environmental issues. The Susa Valley tremolite shows a marked fibrous character, a small reduction of fiber size under grinding, and a consistent increase of the surface area. From the toxicological point of view, such tremolite fibers have been shown to be very effective in the generation of reactive oxygen species. They exhibit a very high cellular reactivity as a consequence of their morphology, structure, and crystal chemistry. Results of combined electron microprobe analysis, Mössbauer spectroscopy, and parallel-beam X-ray powder diffraction are reported for fibrous tremolite from a serpentine-schist from the "Unità Oceanica della Bassa Val di Susa" collected near Condove, Susa Valley, Italy. Data indicate that Fe^{2+} (84% of Fe_{tot}) is located at both the (M1 + M3) and M2 sites and that Fe^{3+} is at M2, in an approximate 3:2:1 ratio, respectively. No evidence of a split M4 site has been observed. The presence of $^{M1+M3}Fe^{2+}$ is confirmed by FTIR spectroscopy to be distributed 70% at M1 and 30% at M3. Both the composition $(Ca_{1.95}K_{0.01}Na_{0.05})_{\Sigma 2.01}$ $(^{VI}Al_{0.01}Fe^{3+}_{0.02}Fe^{2+}_{0.11}Mg_{4.84}Mn_{0.02})_{\Sigma 5.00}Si_{8.00}O_{22}(OH_{1.96}F_{0.03}Cl_{0.01})_{\Sigma 2.00}$ and the cell volume 907.37(1) Å^3 of the fibers are close to those expected for end-member (Ca/Mg = 2/5) tremolite.

Keywords: Fibrous tremolite, amphibole crystal chemistry, Mössbauer spectroscopy, Rietveld method, electron microprobe analysis, Susa Valley, Italy, Trans European Network

INTRODUCTION

In the near future, numerous construction projects are likely to be carried out in northern Italy, all belonging to corridor 5 of the TEN (Trans European Network). In particular, some high-speed railway lines such as Turin-Lyon and Genoa-Milan will involve tunnel excavations occurring in metamorphic formations, such as serpentinites, in which zones containing asbestos minerals may be found. These excavations give rise to worker health and public environmental issues (Piolatto et al. 1990; Astolfi et al. 1991). This contribution is a part of a broad research program devoted to the complete definition of the "amphibole fibers environmental problem" related to the proposed excavation of the Susa Valley railway tunnel. Its goal is to provide up-to-date, clear information to both policy-makers and stakeholders to minimize human exposure to potentially harmful materials. When inhaled, asbestos fibers may give rise to either non-tumor diseases or malignant tumors in the lungs (Martuzzi et al. 1999) and pleura (Mastrantonio et al. 2002). Particular attention should be paid to the effects of asbestos on the rise of pleural mesothelioma (Bignon et al. 1996). The main features of such tumors are particularly long latency, occurrence related to individual susceptibility, a difficult diagnosis, a previous exposure only to asbestos of the amphibole group (Constantopoulos et al. 1987), and most of all, the capability of appearing even after the inhalation of an extremely low asbestos concentration known as triggering dose (U.S. National Research Council 1985; Piolatto 1996). The mechanism through which asbestos fibers may give rise to cancer is not yet completely clear. Many authors agree in attributing the biological activity of the fibers to numerous factors: dimension (Stanton et al. 1981), chemical composition (Fubini 1996; Gilmour et al. 1997), surface properties (Fubini 1993), solubility, and bio persistence (Liu et al. 2000). The diameter and length influence the mechanism of capture and rejection of the fibers. The results of in vitro and in vivo studies show that the longer and thinner fibers are the more dangerous. In fact, the fibers with diameters less than 3 μm and lengths more than 20 μm are partially phagocyted by the alveolar macrophages, with the consequent release of chemical species capable of reacting with the oxygen, causing damage to DNA due to oxidation and modification of the cell's surface. Chemical composition may also contribute to the occurrence of cancer through the presence of iron that may give rise to species capable of reacting with the oxygen, causing the already-mentioned damage. Recent Italian legislation (directives 67/548/CEE and 97/69/CEE) takes into account the above concepts in labeling and classifying carcinogenic

* E-mail: paolo.ballirano@uniroma1.it

agents, focusing particularly on chemical composition (alkaline and terrous-alkaline oxide concentrations), weighted mean diameter, length, and in vivo persistence (i.e., retention of the fibers in the lungs). Characterization of the asbestos minerals extracted during the excavation phases of the construction projects, as well as the development of analytical procedures for an effective characterization of the asbestos hazard, are thus needed.

In the present study, fibrous tremolite from Susa Valley was examined. Tremolite is a monoclinic (*C2/m*), calcic amphibole with a nominal formula of $Ca_2Mg_5Si_8O_{22}(OH)_2$. It is an end-member of the tremolite-ferro-actinolite series. The examined hand specimen is composed of dolomite, tremolite, chlorite, and talc. Tremolite veins contain minor calcite and iron oxides. The specimen comes from a serpentine schist of the "Unità Oceanica della Bassa Val di Susa" of the so-called "Zona Piemontese" Units collected near Condove, Susa Valley. The serpentinites from the Ligurian-Piedmontese formations are usually characterized by a massive structure and fine-grained texture, although they can occur in the form of highly laminated serpentine schists and chlorite schists in tectonic contacts and fault zones. The Alpine metamorphism within these rocks is found prevalently as a serpentinization process. The main mineralogical components are olivine (from which chrysotile asbestos minerals may have formed after its metamorphic modification), clinopyroxene, orthopyroxene, plagioclase, and green spinel. Tremolite is found in localized discontinuities (fault and/or fracture zones), parallel to the direction of movement (slickenside). The veins with the greatest thickness, up to 5 cm, are usually associated with fault movements with extensional components. Tremolite may also be found in extension veins, with an orthogonal direction to the movement along fault fractures connected as the only kinematical link to the extension veins. For a detailed geological outline of the Susa Valley in connection with the project of the Turin-Lyon high-speed railway, see Gattiglio and Sacchi (2006).

The present study is devoted to chemical, structural, and spectroscopic characterization, by combining electron microprobe (EMP) analysis, parallel-beam X-ray powder diffraction (XRPD), ^{57}Fe Mössbauer spectroscopy (MS), and Fourier-transform infrared (FT-IR) spectroscopy, of Susa Valley fibrous tremolite. The aim is to provide detailed crystal-chemical insights to be used to understand the relationships between mineralogical characteristics and biological activity.

Experimental methods

Scanning electron microscopy and electron probe microanalysis

Scanning electron microscopy (SEM) was performed using a FEI Quanta 400 MK2 equipped with an EDAX Genesis EDS system. Images were obtained from a fragment of the hand specimen mounted on a sample stub and carbon coated. Analytical conditions were: 30 kV accelerating voltage, 0.5 nA beam current. Electron micrographs at low and high magnifications are reported in Figure 1. Particle morphologies are restricted to acicular structures, fiber bundles, and rare, very small prismatic crystals (Fig. 1a). Fibers are often curved and may reach centimeter dimensions; width of individual fibrils is generally of the order of 1 μm, but may be as small as 0.2 μm (Fig. 1b).

Bundles of fibers, selected using a binocular microscope, were embedded in epoxy and gently polished with diamond paste to a ¼ μm finish. The composition of tremolite was determined using a Cameca SX50 electron microprobe equipped with five wavelength-dispersive spectrometers using the following conditions: 10 s counting time (peak), 5 s counting time (background), beam diameter 2 μm, excitation voltage 15 kV, specimen current 15 nA. The following standards were used: wollastonite (Si*K*α and Ca*K*α), rutile (Ti*K*α), corundum (Al*K*α), magnetite (Fe*K*α), metallic manganese (Mn*K*α), periclase (Mg*K*α), orthoclase (K*K*α), jadeite (Na*K*α), fluorophlogopite (F*K*α), and sylvite (Cl*K*α). Raw data were corrected online for drift, dead time, and background; matrix correction was performed with a standard ZAF program. Of the total 30 analytical points, only 14 totaled >97 wt% and were therefore used for determining the sample average chemical composition. For the remaining 16, the observed low totals are attributed to the presence of voids between the single fibers arranged in bundles. However, even in these cases the relative abundances of the elements gave crystal-chemical formulae in excellent agreement with those selected. Table 1 shows the averaged chemical composition, observed ranges, and crystal chemical formula normalized on the basis of 24(O + F + Cl). Cations were assigned, following Hawthorne (1981), to the A, B, C, and T group sites, filled according to the order recommended by Leake et al. (1997).

^{57}Fe Mössbauer spectroscopy

The amphibole fibers were gently ground in an agate mortar with acetone and mixed with a powdered acrylic resin to avoid (or reduce) preferred orientation. About 100 mg of sample were available, and Fe total content was close to 1 wt%, so that the absorber was within the limits for the thin absorber thickness described by Long et al. (1983). Data were collected at room

Table 1. Averaged chemical composition, ranges, and mean crystal chemical formula of the fibrous tremolite from Susa Valley, analyzed by EPM (14 analytical points)

Oxides	wt%	Min.–Max. values	Sites and elements	Number of ions (O + F + Cl = 24)
SiO_2	58.51	57.76–58.80	**T**	
TiO_2	0.02	0–0.06	Si	8.003
Al_2O_3	0.05	0.02–0.14	Σ	8.003
FeO_{tot}	1.17	0.65–1.41		
MnO	0.13	0.02–0.20	**C**	
MgO	23.74	23.27–24.55	^{VI}Al	0.008
CaO	13.29	12.61–13.92	Fe^{3+}	0.021
Na_2O	0.20	0.02–0.29	Fe^{2+}	0.113
K_2O	0.04	0–0.08	Mg	4.842
F	0.07	0–0.16	Mn	0.015
Cl	0.03	0–0.09	Ti	0.002
H_2O*	2.15		Σ	5.001 = 62.111 e$^-$
	99.40			
F, Cl = O	0.03		**B**	
Total	99.37		Ca	1.948
			Na	0.053
Fe_2O_3†	0.20	0.12–0.25	K	0.007
FeO†	0.99	0.55–1.18	Σ	2.008 = 39.676 e$^-$
			Ca/ΣM	0.389
			O3	
			OH	1.962
			F	0.030
			Cl	0.009
			Σ	2.001 = 16.119 e$^-$

* Estimated from stoichiometry.
† Partition according to Mössbauer spectroscopy.

temperature, using a conventional spectrometer system operated in constant acceleration mode with a ^{57}Co source of nominal strength of 50 mCi in rhodium matrix, and recorded with a multichannel analyzer using 512 channels. The velocity range −10 to 10 mm/s was used to detect magnetic oxide impurities, in case they were present. To have good statistics, more than 5 million counts per channel were collected. After velocity calibration against a spectrum of high-purity α-iron foil (25 μm thick), the raw data were folded to 256 channels. The spectrum was fit using the Recoil 1.04 fitting program (Lagarec and Rancourt 1998). A first cycle was done fitting pure Lorentzian line shapes: doublet isomer shift (IS) and quadrupole splitting (QS), and sextet magnetic field (H) were refined (as used in most papers from the literature) with excellent results (χ^2 = 1.24 and linewidths up to 0.25 mm/s). In addition, a second refining cycle was done using quadrupole splitting distributions (QSD), following the approach of Gunter et al. (2003), Rancourt (1994a, 1994b), and Rancourt and Ping (1991). Several fitting models with unconstrained parameters—isomer shift (δ_0), coupling parameter (δ_1), center of a Gaussian component (Δ_0), Gaussian width (σ_Δ), and absorption area (A)—were tried to get a best fit. A model based on two sites (1 Fe^{2+} + 1 Fe^{3+}) with two components for Fe^{2+} and a single component for Fe^{3+} was finally chosen (χ^2 = 1.10) because increasing the number of Gaussian components did not change the resulting distribution significantly. Results of both the Lorentzian and the QSD approach were in agreement and this gave us good confidence in the physical correctness of the distribution analysis. Uncertainties were calculated using the covariance matrix and errors were estimated to be approximately ±3% for both Fe^{2+} and Fe^{3+} absorption areas (Table 2).

X-ray powder diffraction

Powder diffraction data were collected on a fully automated parallel-beam Bruker AXS D8Focus diffractometer, operating in transmission mode, equipped with a Peltier-cooled Si(Li) solid state detector. Fibers were ground under ethanol in an agate mortar and subsequently placed in a 0.7 mm diameter borosilicate glass capillary. A compaction of ca. 70% (estimated from X-ray effective absorption measurements) was obtained via an ultrasonic cleaner. An effective absorption measurement was carried out by collecting the transmitted beam through the samples $I_t(E)$ and the incident primary beam $I_0(E)$, both in direct transmission. A preliminary scan indicated the presence of very minor dolomite (included in the Rietveld refinement), traces of iron oxides and calcite (almost undetectable), and serpentine (two main reflections at 12.5 and 25 °2θ removed from the refinement). Rietveld refinement used the GSAS crystallographic suite of programs (Larson and Von Dreele 1985) using the EXPGUI graphical user interface (Toby 2001). The background was fit with a 36-term Chebyshev polynomial of the first kind to model the amorphous contribution arising from the capillary. Peak-shape was fit by the TCH pseudo-Voigt function (Thompson et al. 1987) modified for asymmetry (Finger et al. 1994). Refined variables were GV, and GW (tan θ-dependent and angle-independent, respectively) Gaussian parameters, LX and LY (1/cos θ- and tan θ-dependent) Lorentzian parameters, and S/L and H/L asymmetry parameters (constrained to be equal in magnitude). Starting structural parameters of fibrous tremolite were those of Yang and Evans (1996), whereas those of Ross and Reeder (1992) were selected for dolomite. Isotropic displacement parameters were kept fixed throughout the refinement to the values of reference data. Cell parameters, fractional coordinates for all non-hydrogen atoms, and site scattering for M1, M2, M3, M4, and M4′ were refined for the fibers. Only cell parameters and scale factor were refined for dolomite. Following the same procedure reported in Gianfagna et al. (2007), the geometry of the system was partly constrained under the following conditions: T^{IV}-O × 8 = 1.625(25) Å, O-O × 12 = 2.655(40) Å, $M1^{VI}$-O = 2.08(1) Å, $M2^{VI}$-O = 2.08(5) Å, $M3^{VI}$-O = 2.07(1) Å, $M4^{VIII}$-O = 2.51(15) Å, $M4'^{VIII}$-O = 2.55(35) Å. The weight associated with those observations was progressively reduced to two at the last stages of the refinement. However, after a few cycles of refinement, the *y* fractional coordinates of M4′ moved toward M4 with a corresponding reduction of the occupancy to zero, providing a clear indication of the presence of a nonsplit M4 site. In keeping with the small cationic excess at M4 obtained from EMP analyses (0.01 apfu), the possible

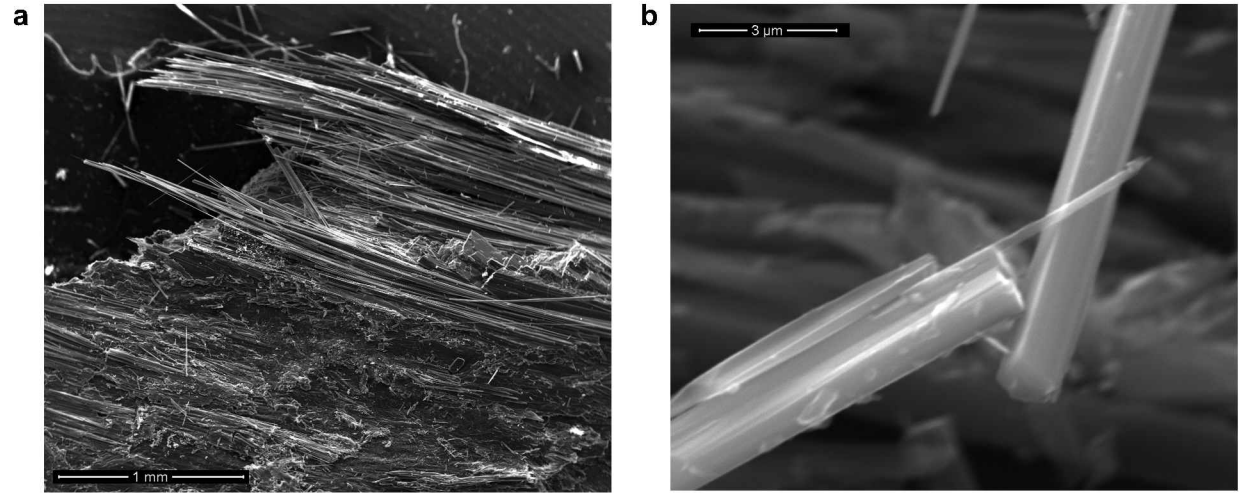

FIGURE 1. SEM images of the Susa Valley tremolite: (**a**) tremolite vein containing minor calcite and iron oxides; (**b**) tremolite fiber with a thinner termination.

TABLE 2. ^{57}Fe Mössbauer hyperfine parameters at room temperature for the fibrous tremolite from Susa Valley

Lineshape	χ^2	Fe^{2+}				Fe^{3+}				Fe^{3+}_{raw} (% Fe_{tot})	Fe^{3+}_{corr} (% Fe_{tot})
		Δ_0 (mm/s)	σ_Δ (mm/s)	δ_0 (mm/s)	Area (%)	Δ_0 (mm/s)	σ_Δ (mm/s)	δ_0 (mm/s)	Area (%)		
Lorentzian	1.24	1.88		1.14	33	0.80		0.20	19	19	16
		2.90		1.13	48						
QSD	1.10	1.90	0.18	1.14	35	0.86	0.40	0.12	20	20	17
		2.88	0.17		45						

Notes: Isomer shift (δ_0) with respect to α-iron. For Quadrupole Splitting Distribution (QSD): $\gamma = 0.194$ mm/s, $\delta_1 = 0$ for both Fe^{3+} and Fe^{2+}; $h_+/h_- = 1$. Symbols according to Rancourt and Ping (1991). Fe^{3+}_{raw} is just the area of absorption peaks assigned to Fe^{3+}, while Fe^{3+}_{corr} is obtained from Fe^{3+}_{raw} by applying the correction factor C = 1.22 (Dyar et al. 1993). Estimated uncertainties are about 0.02 mm/s for hyperfine parameters, and no less than 3% for absorption areas.

occurrence of a partly occupied A site was also investigated. However, attempts to detect electron density at A, A*m*, and A2 were unsuccessful.

Attempts to model the presence of preferred orientation by means of the generalized spherical harmonics description of Von Dreele (1997) produced a small improvement of the fit as a result of a J texture index of 1.122. Convergence was reached at R_p = 5.64%, R_{wp} = 7.35%, R_F = 3.35%, reduced χ^2 = 1.96, contribution of the restraints to χ^2 = 83.2. Experimental details and other data of the refinement are reported in Table 3, cell parameters and site scattering (s.s.) values in Table 4, fractional coordinates and isotropic displacement parameters in Table 5, selected bond distances in Table 6, and experimental, calculated, and difference plots are displayed in Figure 2.

Fourier transform infrared spectroscopy

FTIR data were collected on a Perkin Elmer Spectrum One over the range 4000–400 cm^{-1}: 64 scans at a nominal resolution of 4 cm^{-1} were averaged. The instrument was equipped with a KBr beamsplitter and a TGS detector. The powdered sample was mixed in a 2:100 ratio with 200 mg of KBr to obtain a transparent pellet. Measurement was done at room temperature.

RESULTS AND DISCUSSION

Crystal chemistry

Inspection of the various EPM analyses suggests that the fibers present chemical homogeneity. This is confirmed by the absence of relevant peak-broadening and/or asymmetry of the X-ray powder diffraction pattern. The lowest alkali content is related to the largest Ca content. FeO_{tot} content spans a range from 0.65 to 1.41 wt%, but no correlation between Ca and Fe content was observed. This fact seems to indicate the absence of a Ca $\leftrightarrow$ $^{M4}Fe^{2+}$substitution scheme.

The Mössbauer spectrum of fibrous tremolite from Susa Valley is typical of a paramagnetic material with some accessory magnetic phases, the latter accounting for about 29% of total Fe (Fig. 3). The magnetic phases were identified as hematite (IS = 0.39 mm/s, H = 51 T, 19% of Fe_{tot}) and magnetite (IS = 0.30 and 0.77 mm/s, H = 51 and 46 T, respectively, 10% of Fe_{tot}) and their contribution to the absorption spectrum was subtracted from the $\%Fe^{3+}$ of the amphibole. The spectrum of fibrous tremolite is well-represented by three quadrupole doublets: the first two show IS values of about 1.1 mm/s and QS values of about 1.9 and 2.9 mm/s, and were assigned to Fe^{2+}; the third shows an IS of about 0.2 mm/s and a QS of about 0.8 mm/s, and was assigned to Fe^{3+} (Table 2). A very close match was observed between the results of Lorentzian and QSD analysis. Fe^{3+} proportions are quantified at 19% Fe_{tot} from direct area measurement (Fe^{3+}_{raw}) and 16% when adjusting for the recoil-free fraction (Fe^{3+}_{corr}), as suggested by Dyar et al. (1993).

In the case of the tremolite-actinolite series, Burns and

TABLE 3. Experimental details of the X-ray powder diffraction data collection and miscellaneous data of the refinement

Instrument	Bruker AXS D8 Focus
X-ray tube	Cu at 40 kV and 40 mA ($CuK\alpha_1$ = 1.540598 Å)
Incident beam optic	Multilayer X-ray mirrors
Sample mount	Rotating capillary (30 rpm)
Soller slits	2 (2.3° divergence)
Divergence and antidivergence slits	1 mm
Detector slit	0.2 mm (0.1°)
Detector	Peltier-cooled solid state Si(Li) SolX
2θ range (°)	5–155 (7501 data points)
Step size (°)	0.02
Counting time (s)	30
R_p (%), R_{wp} (%), R_F (%)	5.64, 7.35, 3.35
Reduced χ^2	1.964
Restraints contribution to χ^2	83.2
Refined parameters	97
Peak cut-off (%)	0.02
J	1.122
GV, GW	45(2), 21.7(6)
LX, LY	0.6(1), 3.0(3)
S/L = H/L	0.0238(2)
Amphibole wt%	99.644(3)
Dolomite wt%	0.36(3)

Note: Statistical descriptors as defined by Young (1993).

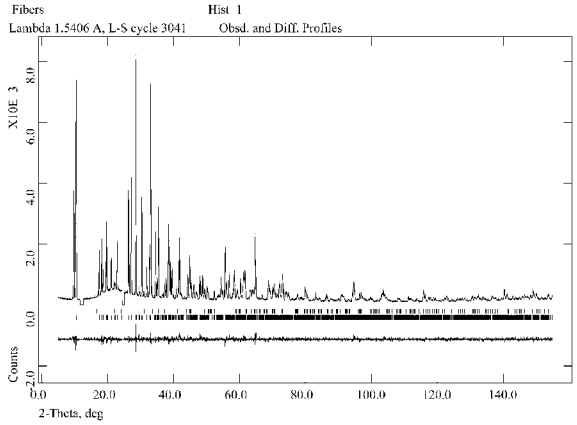

FIGURE 2. Experimental (dots), calculated (solid line), and difference plots of the Rietveld refinement of the fibrous tremolite from Susa Valley. Vertical markers refer, from above to below, to calculated Bragg reflections of dolomite and tremolite. Two peaks of serpentine at 12.5 and 25 °2θ were removed from calculation.

TABLE 4. Unit-cell parameters and site scattering values (in electrons per formula unit) for the fibrous tremolite from Susa Valley obtained from the structure refinement

	Refinement	Possible site partition	Chemical data
a (Å)	9.84174(8)	–	–
b (Å)	18.05932(19)	–	–
c (Å)	5.27876(6)	–	–
β (°)	104.732(1)	–	–
V (Å^3)	907.37(1)	–	–
M4	40.20(12)	$Ca_{1.95}$;$Na_{0.05}$;$K_{0.01}$	(39.68)
Sum B sites	40.20	–	39.68
M1	24.98(14)	$Al_{0.01}$; $Fe^{2+}_{0.05}$;$Mg_{1.92}$;$Mn_{0.02}$	(24.97)
M2	24.50(14)	$Fe^{2+}_{0.04}$;$Fe^{3+}_{0.02}$;$Mg_{1.94}$	(24.84)
M3	12.19(10)	$Fe^{2+}_{0.02}$;$Mg_{0.98}$	(12.28)
Sum C sites	61.67	–	62.09

Note: Possible site partition is the result of combining chemical, Mössbauer, and Rietveld refinement data.

TABLE 5. Fractional coordinates and isotropic displacement parameters (not refined) for the fibrous tremolite from Susa Valley

Site	*x*	*y*	*z*	U_{iso} (Å^2)
O1	0.1139(4)	0.08679(24)	0.2178(10)	0.008
O2	0.1166(5)	0.17198(25)	0.7236(10)	0.008
O3	0.1085(5)	0	0.7137(12)	0.008
O4	0.3657(5)	0.24749(23)	0.7897(12)	0.008
O5	0.3454(5)	0.13364(23)	0.0985(11)	0.008
O6	0.3438(5)	0.11794(21)	0.5950(11)	0.008
O7	0.3387(6)	0	0.2893(15)	0.008
T1	0.28106(22)	0.08436(12)	0.2977(5)	0.005
T2	0.28751(25)	0.17064(11)	0.8041(6)	0.005
M1	0	0.08738(18)	0.5	0.007
M2	0	0.17656(20)	0	0.007
M3	0	0	0	0.007
M4	0	0.27737(12)	0.5	0.007
H	0.206*	0	0.771*	0.030

* Fractional coordinates, taken from Yang and Evans (1996), unrefined.

Greaves (1971) attributed the Fe^{2+} doublets with QS of 1.7–1.9 and 2.8–2.9 mm/s to the presence of $^{M2}Fe^{2+}$ and $^{M1}Fe^{2+}$, respectively. More recently, many authors agreed to assign the doublet with lowest QS to $^{M2}Fe^{2+}$, but different assignments were proposed for the doublets with highest QS, often suggesting an irresolvable combination of $^{M1+M3}Fe^{2+}$ (see Gunter et al. 2003 and references therein).

In the present work, according to the area of the Mössbauer absorption peaks, Fe^{2+} was preliminarily allocated at M2 (QS of 1.88 mm/s, 40% of the total Fe^{2+}) and at M1 + M3 (QS of 2.90 mm/s, 60% of the total Fe^{2+}). Moreover, the Fe^{3+} was assigned to represent occupancy at the M2 site, as consistently reported by various authors for sodic amphiboles (Ernst and Wai 1970), strontian potassirichterite (Sokolova et al. 2000), ferrian winchite (Sokolova et al. 2001), winchite-richterite (Gunter et al. 2003), and fluoro-edenite (Gianfagna et al. 2007). Combining chemical data and Mössbauer $Fe^{3+}/\Sigma Fe$ ratios we obtain the following average composition: SiO_2 58.51%, TiO_2 0.02%, Al_2O_3 0.05%, Fe_2O_3 0.20%, MgO 23.74%, CaO 13.29%, MnO 0.13%, FeO 0.99%, Na_2O 0.20%, K_2O 0.04%, F 0.07%, Cl 0.03%, H_2O 2.15% (estimated content to obtain a total of 2 OH + F + Cl apfu), and the corresponding chemical formula: $(Ca_{1.95}K_{0.01}Na_{0.05})_{\Sigma 2.01}$ $(^{VI}Al_{0.01}Fe^{3+}_{0.02}Fe^{2+}_{0.11}Mg_{4.84}Mn_{0.02})_{\Sigma 5.00}Si_{8.00}O_{22}(OH_{1.96}F_{0.03}Cl_{0.01})_{\Sigma 2.00}$. Therefore, the sample represents a nearly ideal tremolite (Ca/ΣM = 0.389; M = Mg + Fe^{2+} + Mn + Ni + Ti + $^{VI}Fe^{3+}$ + $^{VI}Cr^{3+}$ + ^{VI}Al), and Mg = 0.98 [Mg = Mg/(Mg + Fe^{2+})].

The measured cell volume of 907.37(1) Å^3 compares favorably with values of 906.5 Å^3 (Gottschalk et al. 1999), 906.6 Å^3 (Verkouteren and Wylie 2000), and 907.0 Å^3 (Yang and Evans 1996) reported for pure tremolite (Ca/Mg = 2/5). Moreover, it takes into account the presence of 2.2% ferroactinolite content [X_{FeA} =(Fe^{2+} + Mn)/(Fe^{2+} + Mn + Mg)]. In particular, the chemical composition and cell parameters of the fibers are close to samples 9 and 31 of Verkouteren and Wylie (2000).

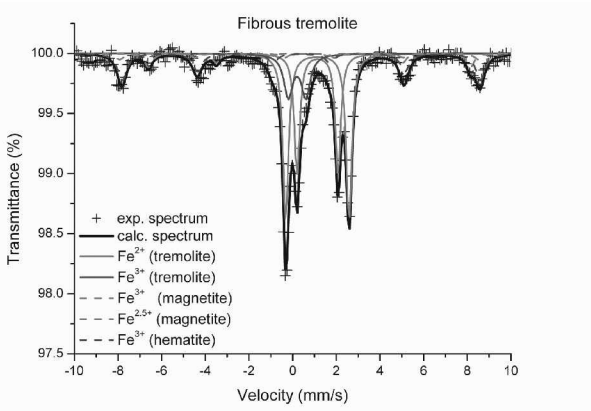

FIGURE 3. Room-temperature ^{57}Fe Mössbauer spectrum of fibrous tremolite sample from Susa Valley. Magnetic iron oxides were revealed and subtracted from the Fe^{3+}/Fe_{tot} ratio calculation.

Rietveld refinement indicates very marginal differences in bond distances relative to the reference data of Yang and Evans (1996). The mean T1-O distance is slightly smaller than T2-O reported for *C*2/*m* amphiboles with no tetrahedrally coordinated Al (Hawthorne 1981). Polyhedral distortion Δ shows comparable values for both T1- and T2-centered tetrahedra. Site scattering of M1, M2, and M3 sites consistently indicates the minor presence of a scatterer heavier than Mg in agreement with both chemical data and the assignment of Mössbauer spectroscopy. A possible site assignment is proposed in Table 4. A remarkably good agreement is observed between site scattering derived from Rietveld refinement and those from chemical data, largest differences being smaller than 1.5%. This is fully consistent with the findings of previous works on fibrous amphiboles (Gianfagna et al. 2003, 2007). Site partitioning, beside the constraints indicated by Mössbauer spectroscopy, allocates 70% of the $^{M1+M3}Fe^{2+}$ at M1 and 30% at M3, to fulfill the requirement of only a slightly increased s.s. at M3 with respect to that of a Mg atom. Therefore, considering site multiplicity, nearly equal distribution of Fe^{2+} may be observed over each one of the sites M1, M2, and M3 (Table 4), with a small preference for M1, consistent with the findings of Evans and Yang (1998) for the tremolite – actinolite – ferro-actinolite series.

The presence of $^{M1+M3}Fe^{2+}$ is confirmed by FTIR spectroscopy (Fig. 4). In fact, besides the typical tremolite absorption band at 3673–3675 cm^{-1} assigned to the vibration of the O-H dipole bonded to three ^{VI}Mg cations, a well-developed band is observed at 3660 cm^{-1}. This latter was attributed to the $^{M1+M3}Fe^{2+}$ environment, according to results of Skogby and Rossman (1991). Moreover, no $^{M1+M3}Fe^{+3}$ is present because absorption bands at Δ = –50 cm^{-1} from the tremolite reference band (Raudsepp et al. 1987) are absent. No A cation is observed either, as would be indicated by absorption bands at Δ = +55–60 cm^{-1} (Robert et al. 1989).

TABLE 6. Selected bond distances (Å) and polyhedral distortion ($\Delta \times 10^4$) for the fibrous tremolite from Susa Valley

	Present work	YE96		Present work	YE96
T1-O1	1.592(4)	1.600(1)	T2-O2	1.627(4)	1.612(1)
T1-O5	1.624(5)	1.633(1)	T2-O4	1.598(4)	1.587(1)
T1-O6	1.649(5)	1.630(2)	T2-O5	1.654(6)	1.656(2)
T1-O7	1.630(2)	1.619(1)	T2-O6	1.656(5)	1.676(1)
<T1-O >	1.624	1.620	<T2-O >	1.634	1.633
Δ	1.6	0.6	Δ	2.1	4.6
M1-O1 × 2	2.080(5)	2.067(1)	M2-O1 × 2	2.133(5)	2.134(1)
M1-O2 × 2	2.087(5)	2.081(1)	M2-O2 × 2	2.074(5)	2.088(1)
M1-O3 × 2	2.071(4)	2.087(1)	M2-O4 × 2	2.028(5)	2.019(1)
<M1-O>	2.079	2.078	<M2-O>	2.078	2.080
Δ	0.1	0.2	Δ	4.3	5.2
M3-O1 × 4	2.093(4)	2.073(1)	M4-O2 × 2	2.375(5)	2.405(1)
M3-O3 × 2	2.060(6)	2.062(2)	M4-O4 × 2	2.306(5)	2.327(1)
<M3-O>	2.082	2.069	M4-O5 × 2	2.784(5)	2.766(2)
Δ	0.6	0.1	M4-O6 × 2	2.565(4)	2.535(2)
			<M4-O>	2.508	2.508
			Δ	55	44

Note: Polyhedral distortion Δ as defined by Brown and Shannon (1973): $\Delta = \frac{1}{n}\sum\left(\frac{R_i - \overline{R}}{\overline{R}}\right)^2$ where n is the number of ligands, $\overline{R}$ is the average bond length and R_i an individual bond length. Reference data of Yang and Evans (1996) (YE96) from single-crystal analysis are reported for comparison purposes.

No correlations between mean bond distances <M1-O>, <M2-O>, and <M3-O> have been attempted because their differences are within the standard deviation of individual bond distances, which gave uncertainties on the mean cationic radius $<r_M>$ of 0.005Å (see also Fig. 1 in Evans and Yang 1998). However, the combined increase of both <M3-O> and Δ with respect to ideal tremolite (Yang and Evans 1996) is consistent with the presence of $^{M3}Fe^{2+}$.

Environmental and toxicological relevance

The problem of human exposure to airborne mineral dusts in daily life has recently become more and more relevant. Among those related to amphibole fibers, the examples of Libby (Montana, U.S.A.) and Biancavilla (Sicily, Italy) are well documented (Gunter et al. 2007 and references therein). The case of Susa Valley (Italy) is, in some aspects, even more peculiar because in addition to the epidemiological investigation related to environmental exposure to fibers, there is a need for a prediction of excavation effects focusing, in particular, on the amount of fiber released into the environment.

The harmful potential of Susa Valley tremolite on human health was recently shown to be very high. With respect to other fibrous tremolites of the Western Alps, it shows a small reduction of fibrousness and a consistent increase of the surface area under grinding. Moreover, from the toxicological point of view, such tremolite has been proved to be very effective in the generation of reactive oxygen species (ROS) and in the activation of biological reactivity (Turci et al. 2007). Mineral-induced ROS has been observed to determine a strong release of •OH free radicals, whose generation may be explained via an iron-catalyzed Haber-Weiss cycle (Fubini and Otero Aréan 1999):

$$\text{Reductant} + Fe^{3+} \rightarrow \text{oxidized reductant} + Fe^{2+};$$
$$Fe^{2+} + O_2 \rightarrow Fe^{3+} + O_2^{\bullet -};$$
$$O_2^{\bullet -} + 2H^+ + e^- \rightarrow H_2O_2;$$
$$Fe^{2+} + H_2O_2 \rightarrow Fe^{3+} + OH^- + {}^{\bullet}OH.$$

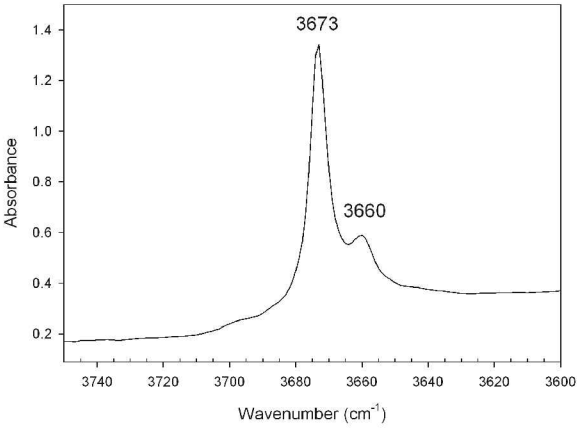

FIGURE 4. FT-IR spectrum in the 3750–3600 cm^{-1} wavenumber range.

The role of free radicals in inducing DNA damage and subsequent carcinogenesis is well recognized in scientific literature. However, in the case of tremolite this is not the only mechanism because iron content is generally small as compared to, for example, Libby winchite (Meeker et al. 2003; Gunter et al. 2003) and Biancavilla fluoro-edenite (Gianfagna et al. 2007). Cytotoxicity of Susa Valley tremolite on A549 lung cells has been shown to be comparable to cytotoxicity of crocidolite: this is due to its oxidative stress, measured from release of LDH enzyme, as well as to its inhibition of anti-oxidative defenses, measured from the reduction of the pentose phosphate pathway (Gazzano et al. 2007). According to these very challenging findings, the cytotoxic/oncogenic pathway following the tremolite/cell interaction seems to be dependent on different fiber morpho-structural and crystal-chemical features as well as on surface chemistry. Therefore, a full characterization (morphology, resistance to comminution, crystal structure, crystal chemistry, Fe^{3+}/Fe_{tot} ratio, cation site partitioning) of different fibrous amphiboles coupled with both in vitro and in vivo analyses (to determine their cytotoxicity) would be useful.

ACKNOWLEDGMENTS

This research was carried out within CNR-IGAG and CNR-IGG research priorities and under the financial support of Università di Roma "La Sapienza." Thanks are due to Elena Spaziani for help in FTIR data acquisition.

REFERENCES CITED

Astolfi, A., Belluso, E., Ferraris, G., Fubini, B., Giamello, E., and Volante, M. (1991) Asbestiform minerals associated with chrysotile from Western Alps (Piedmont-Italy): Chemical characteristics and possible related toxicity. In R.C Brown, J.A. Hoskins, and N.F. Johnson, Eds., Mechanisms in Fiber Carcinogenesis, 223, p. 269–283. NATO ASI Series A: Life Sciences, Plenum Press, New York.

Bignon, L., Brochard, P., and Pairon, L.C. (1996) Mesothelioma: causes and fiber-related mechanism. In J. Aisner, M.C. Perry, and M.R. Green, Eds., Comprehensive textbook of thoracic oncology, p. 735–756. Lippincott, Williams, and Wilkins, Baltimore.

Brown, I.D. and Shannon, R.D. (1973) Empirical bond-strength-bond-length curves for oxides. Acta Crystallographica, A29, 266–282.

Burns, R.G. and Greaves, C. (1971) Correlations of infrared and Mössbauer site population measurements of actinolites. American Mineralogist, 56, 2010–2033.

Constantopoulos, S.H., Saratzis, N.A., Kontogiannis, D., Karantanas, A., Goudevenos, J.A., and Katsiotis, P. (1987) Tremolite whitewashing and pleural calcifications. Chest, 92, 709–712.

Dyar, M.D., Mackwell, S.M., McGuire, A.V., Cross, L.R., and Robertson, J.D. (1993) Crystal chemistry of Fe^{3+} and H^+ in mantle kaersutite: Implications for mantle metasomatism. American Mineralogist, 78, 968–979.

Ernst, W.G. and Wai, C.N. (1970) Mössbauer, infrared, X-ray, and optical study of cation ordering and dehydrogenation in natural and heat-treated sodic amphiboles. American Mineralogist, 55, 1226–1258.

Evans, B.W. and Yang, H. (1998) Fe-Mg order-disorder in tremolite-actinolite-ferro-actinolite at ambient and high temperature. American Mineralogist, 83, 458–475.

Finger, L.W., Cox, D.E., and Jephcoat, A.P. (1994) A correction for powder diffraction peak asymmetry due to axial divergence. Journal of Applied Crystallography, 27, 892–900.

Fubini B. (1993) The possible role of surface chemistry in the toxicity of inhaled fibers. In D.B. Wahreit, Ed., Fiber Toxicology, 11, p. 229–257. Academic Press, San Diego.

——— (1996) Physico-chemical and cell free assays to evaluate the potential carcinogenicity of fibres. In A.B. Kane, P. Boffetta, R. Saracci, and J. Wilbourn, Eds., Mechanisms of fiber carcinogenesis, IARC Scientific Publication 140. International Agency for Research on Cancer, Lyon.

Fubini, B. and Otero Aréan, C. (1999) Chemical aspects of the toxicity of invale mineral dusts. Chemical Society Reviews, 28, 373–381.

Gattiglio, M. and Sacchi, R. (2006) Lineamenti geologici della Val di Susa lungo il tracciato del progetto TAV Torino-Lione. Rendiconti della Società Geologica Italiana, 3, 13–19 (in Italian).

Gazzano, E., Turci, F., Riganti, C., Tomatis, M., Fubini, B., Bosia, A., and Ghigo, D. (2007) La tremolite nelle alpi occidentali: test cellulari con prospettive tossicologiche. Workshop "Anfiboli fibrosi: nuove problematiche relative al rischio ambientale e sanitario." Roma, 27–28 April 2007, Abstracts, 73–74 (in Italian).

Gianfagna, A., Ballirano, P., Bellatreccia, F., Bruni, B.M., Paoletti, L., and Oberti, R. (2003) Characterization of amphibole fibers linked to mesothelioma in the area of Biancavilla, Eastern Sicily, Italy. Mineralogical Magazine, 67, 1221–1229.

Gianfagna, A., Andreozzi, G.B., Ballirano, P., Mazziotti-Tagliani, S., and Bruni, B.M. (2007) Structural and chemical contrasts between prismatic and fibrous fluoro-edenite from Biancavilla, Sicily, Italy. Canadian Mineralogist, 45, 249–262.

Gilmour, P.S., Brown, D.M., Beswik, P.H., Macnee, W., Rahman, I., and Donaldson, K. (1997) Free radical activity of industrial fibers: Role of iron in oxidative stress and activation of transcription factors. Environmental Health Perspectives, 105 Suppl. 5, 1313–1317.

Gottschalk, M., Andrut, M., and Melzer, S. (1999) The determination of the cummingtonite content of synthetic tremolite. European Journal of Mineralogy, 11, 967–982.

Gunter, M.E., Dyar, M.D., Twamley, B., Foit, Jr., F.F., and Cornelius, C. (2003) Composition, $Fe^{3+}/\Sigma Fe$, and crystal structure of non-asbestiform and asbestiform amphiboles from Libby, Montana, U.S.A. American Mineralogist, 88, 1970–1978.

Gunter, M.E., Belluso, E., and Mottana, A. (2007) Amphiboles: Environmental and health concerns. In F.C. Hawthorne, R. Oberti, G. Della Ventura, and A. Mottana, Eds., Amphiboles: Crystal Chemistry, Occurrence, and Health Issues, 67, p. 453–516. Reviews in Mineralogy and Geochemistry, Mineralogical Society of America, Chantilly, Virginia.

Hawthorne, F.C. (1981) Crystal chemistry of the amphiboles. In D.R. Veblen, Ed., Amphiboles and Other Hydrous Pyriboles—Mineralogy, 9A, p. 1–102. Reviews in Mineralogy, Mineralogical Society of America, Chantilly, Virginia.

Lagarec, K. and Rancourt, D.G. (1998) RECOIL. Mössbauer spectral analysis software for Windows, version 1.0. Department of Physics, University of Ottawa, Canada.

Larson, A.C. and Von Dreele, R.B. (1985) General structure analysis system (GSAS). Los Alamos National Laboratory Report LAUR 86–748.

Leake, B.E., Woolley, A.R., Arps, C.E.S., Birch, W.D., Gilbert, M.C., Grice, J.D., Hawthorne, F.C., Kato, A., Kisch, H.J., Krivovichev, V.G., Linthout, K., Laird, J., Mandarino, J.A., Maresch, V.W., Nickel, E.H., Rock, N.M.S., Schumacher, J.C., Smith, D.C., Stephenson, N.N., Ungaretti, L., Whittaker, E.J.W., and Youzhi, G. (1997) Nomenclature of amphiboles: Report of the subcommittee on amphiboles of the International Mineralogical Association, Commission on New Minerals and Mineral Names. American Mineralogist, 82, 1019–1037.

Liu, W., Ernst, J.D., and Broaddus, V.C. (2000) Phagocytosis of crocidolite asbestos induces oxidative stress, DNA damage, and apoptosis in mesothelial cells. American Journal of Respiratory Cell and Molecular Biology, 23, 371–378.

Long, G.J., Cranshaw, T.E., and Longworth, G. (1983) The ideal Mössbauer effect absorber thickness. Mössbauer Effect Reference Data Journal, 6, 42–49.

Martuzzi, M., Comba, P., De Santis, M., Lavarone, I., Di Paola, M., Mastrantonio, M., and Pirastu, R. (1999) Asbestos-related lung cancer mortality in Piedmont, Italy. American Journal of Industrial Medicine, 33, 565–570.

Mastrantonio, M., Belli, S., Binazzi, A., Carboni, M., Comba, P., Fusco, P., Grignoli, M., Lavarone, I., Martuzzi, M., Nesti, M., Trinea, S., and Uccelli, R. (2002) Istituto Superiore di Sanità. La mortalità per tumore maligno della pleura nei comuni italiani (1988–1997) Rapporti ISTISAN 02/12, 27 p. (in Italian).

Meeker, G.P., Bern, A.M., Brownfield, I.K., Lowers, H.A., Sutley, S.J., Hoefen, T.M., and Vance, J.S. (2003) The composition and morphology of amphiboles from the Rainy Creek Complex, near Libby, Montana. American Mineralogist, 88, 1955–1969.

Piolatto, G. (1996) Valori di riferimento e valori limite per l'amianto, In C. Aprea, G. Sciarra, M.L. Fiorentino, and C. Minoia, Eds., I valori di riferimento e i valori limite nella prevenzione ambientale e occupazionale, p. 153–161. Morgan Edizioni Tecniche, Milano (in Italian).

Piolatto, G., Negri, E., La Vecchia, C., Pira, E., Decarli, A., and Peto, J. (1990) An update of cancer mortality among crysotile asbestos miners in Balangero, Northern Italy. British Journal of Industrial Medicine, 47, 810–814.

Rancourt, D.G. (1994a) Mössbauer spectroscopy of minerals. I. Inadequacy of Lorentzian-line doublets in fitting spectra arising from quadrupole splitting distributions. Physics and Chemistry of Minerals, 21, 244–249.

——— (1994b) Mössbauer spectroscopy of minerals. II. Problem of resolving *cis* and *trans* octahedral Fe^{2+} sites. Physics and Chemistry of Minerals, 21, 250–257.

Rancourt, D.G. and Ping, J.Y. (1991) Voigt-based methods for arbitrary-shape static hyperfine parameter distributions in Mössbauer spectroscopy. Nuclear Instruments and Methods in Physics Research, B58, 85–97.

Raudsepp, M., Turnock, A.C., Hawthorne, F.C., Sherriff, B.K., and Hartman, J.S. (1987) Characterization of synthetic pargasitic amphiboles ($NaCa_2Mg_4M^{3+}Si_6Al_2O_{22}(OH,F)_2$; M^{3+} = Al, Cr, Ga, Sc, In) by infrared spectroscopy, Rietveld structure refinement, and ^{27}Al, ^{29}Si, and ^{19}F MAS NMR spectroscopy. American Mineralogist, 72, 580–593.

Robert, J.-L., Della Ventura, G., and Thauvin, J.-L. (1989) The infrared OH-stretching region of synthetic richterites in the system Na_2O-K_2O-CaO-MgO-SiO_2-H_2O-HF. European Journal of Mineralogy, 1, 203–211.

Ross, N.L. and Reeder, R.J. (1992) High-pressure structural study of dolomite and ankerite. American Mineralogist, 77, 412–421.

Skogby, H. and Rossman, G.R. (1991) The intensity of amphibole OH bands in the Infrared absorption spectrum. Physics and Chemistry of Minerals, 18, 64–68.

Sokolova, E.V., Kabalov, Y.K., McCammon, C., Schneider, J., and Konev, A.A. (2000) Cation partitioninig in an unusual strontian potassicrichterite from Siberia: Rietveld structure refinement and Mössbauer spectroscopy. Mineralogical Magazine, 64, 19–23.

Sokolova, E.V., Hawthorne, F.C., McCammon, C., and Schneider, J. (2001) Ferrian winchite from the Ilmen Mountains, Southern Urals, Russia and some problems with the current scheme of nomenclature. Canadian Mineralogist, 39, 171–177.

Stanton, M.F., Layard, M., Tegeris, A., Miller, E., May, M., Morgan, E., and Smith, A. (1981) Relation of particle dimension to carcinogenicity in amphibole asbestoses and other fibrous minerals. Journal of the National Cancer Institute, 67, 965–975.

Thompson, P., Cox, D.E., and Hastings, J.B. (1987) Rietveld refinement of Debye-Scherrer synchrotron X-ray data from Al_2O_3. Journal of Applied Crystallography, 20, 79–83.

Toby, B.H. (2001) EXPGUI, a graphical user interface for GSAS. Journal of Applied Crystallography, 34, 210–213.

Turci, F., Gazzano, E., Tomatis, M., Riganti, C., Ghigo, D., and Fubini, B. (2007) La tremolite nelle alpi occidentali: un'analisi chimico-fisica con prospettive tossicologiche. Workshop "Anfiboli fibrosi: nuove problematiche relative al rischio ambientale e sanitario." Roma, 27–28 April 2007, Abstracts, 68–72 (in Italian).

U.S. National Research Council (1985) Asbestiform fibres: Non-occupational health risks, 352 p. National Academy Press, Washington.

Verkouteren, J.R. and Wylie, A.G. (2000) The tremolite-actinolite-ferro-actinolite series: Systematic relationship among cell parameters, composition, optical properties, and habit, and evidence of discontinuities. American Mineralogist, 85, 1239–1254.

Von Dreele, R.B. (1997) Quantitative texture analysis by Rietveld refinement. Journal of Applied Crystallography, 30, 517–525.

Yang, H. and Evans, B.W. (1996) X-ray structure refinements of tremolite at 140 and 295 K: Crystal chemistry and petrologic implications. American Mineralogist, 81, 1117–1125.

Young, R.A. (1993) Introduction to the Rietveld method. In R.A. Young, Ed., The Rietveld Method, p. 1–38. Oxford Science, U.K.

MANUSCRIPT RECEIVED NOVEMBER 26, 2007
MANUSCRIPT ACCEPTED FEBRUARY 19, 2008
MANUSCRIPT HANDLED BY DARBY DYAR